BIOCHEMISTRY
including biophysical chemistry & molecular biology

Article

pubs.acs.org/biochemistry

Structural Analysis of Calmodulin Binding by nNOS Inhibitory Amphibian Peptides

Antonio N. Calabrese, John H. Bowie, and Tara L. Pukala*

School of Chemistry and Physics, The University of Adelaide, Adelaide, SA Australia 5005

Supporting Information

ABSTRACT: Calmodulin (CaM) is a ubiquitous protein in nature and plays a regulatory role in numerous biological processes, including the upregulation of nitric oxide (NO) synthesis in vivo. Several peptides that prevent NO production by interacting with CaM have been isolated in the cutaneous secretions of Australian amphibians, and are thought to serve as a defense mechanism against predators. In this work, we probe the mechanism by which three of these peptides, namely, caerin 1.8, dahlein 5.6, and a synthetic modification of citropin 1.1, interact with CaM to inhibit NO signaling. Isothermal titration calorimetry was used to determine thermodynamic parameters of the binding interactions and revealed that all the peptides bind to CaM in a similar fashion, with the peptide encapsulated between the two lobes of CaM. Ion mobility-mass spectrometry was used to investigate the changes in collision cross section that occur as a result of complexation, providing additional evidence for this binding mode. Finally, nuclear magnetic resonance spectroscopy was used to track chemical shift changes upon binding. The results obtained confirm that these complexes adopt canonical collapsed structures and demonstrate the strength of the interaction between the peptides and CaM. An understanding of these molecular recognition events provides insights into the underlying mechanism of the amphibian host-defense system.

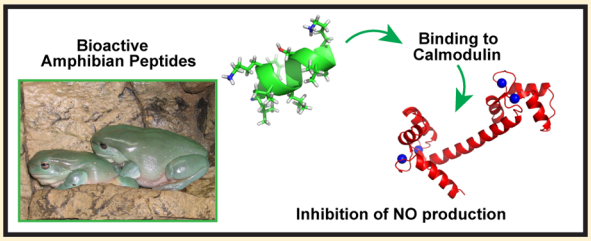

The anuran (frog and toad) skin is a complex organ that performs numerous functions necessary for the animal's survival, including respiration, thermoregulation, and self-defense.[1] Importantly, secretions of the granular glands are a vital component of the animal's defense arsenal, and are vital to ensure they survive in the hostile environment in which they live. Several classes of biologically active peptides have been identified in secretions of the cutaneous glands of Australian anurans, including wide-spectrum antimicrobials, anticancer active peptides, and neuropeptides.[2−4]

Most amphibians of the genera *Litoria* and *Crinia* that have been studied thus far produce one or more peptide(s) that inhibit the production of nitric oxide (NO) by neuronal nitric oxide synthase (nNOS) as part of their glandular secretion, with studies identifying more than 50 such peptides.[2,3,5] It is thought that peptides of this type may play a regulatory role in the animals, as it is known that NO is involved in anuran sight, gastric modulation, and reproduction.[6−8] Additionally, the peptides may also form an integral part of the animal's self-defense mechanisms by interfering with NO signaling in an attacking predator or pathogen.[5] A thorough and complete analysis of the amphibian integument and its roles in both physiological regulation and self-defense is vital to ensure the continued survival of declining amphibian populations worldwide.

NO production is tightly regulated by the protein calmodulin (CaM), a Ca^{2+} binding protein that is one of the cofactors required to facilitate NO production by nNOS.[5] CaM is a small, ubiquitous, highly conserved regulatory protein that is involved in many Ca^{2+}-dependent processes in most eukaryotic cells.[9,10] It is able to perform its regulatory function due to its ability to act as a cytosolic Ca^{2+} sensor and bind four Ca^{2+} ions in a cooperative fashion with high affinity (K_d from 10^{-7} to 10^{-11} M).[9,11,12] This triggers a conformational change to the active configuration (holo-CaM, $Ca^{2+}{}_4$CaM, Figure 1a), revealing hydrophobic patches which allow CaM to associate with its target proteins/peptides.

Target binding by $Ca^{2+}{}_4$CaM triggers significant conformational changes in the regulatory protein.[13] The complex which forms typically belongs to one of two structural classes, namely, collapsed or extended. The canonical collapsed structure is more compact than $Ca^{2+}{}_4$CaM, and its formation is largely driven by hydrophobic interactions between the anchor residues of the binding partner and the hydrophobic binding cavity formed when the N- and C-terminal regions of $Ca^{2+}{}_4$CaM come together in space.[14−17] Electrostatic interactions also contribute to the binding event at the outlets of the hydrophobic cavity, which determine the orientation of the bound target.[14] A number of complexes of this type have been reported in the literature;[18−21] one example is illustrated in Figure 1b. The two lobes of $Ca^{2+}{}_4$CaM do not always engulf their target, and in some instances the protein remains in a relatively extended conformation.[14] For example, in the case of the CaM binding peptide from the plasma membrane Ca^{2+}-pump (C20W), the peptide is bound by only the C-terminal

Received: April 7, 2014
Revised: November 24, 2014
Published: December 1, 2014

DOI: 10.1021/bi5004124
Biochemistry 2015, 54, 567−576

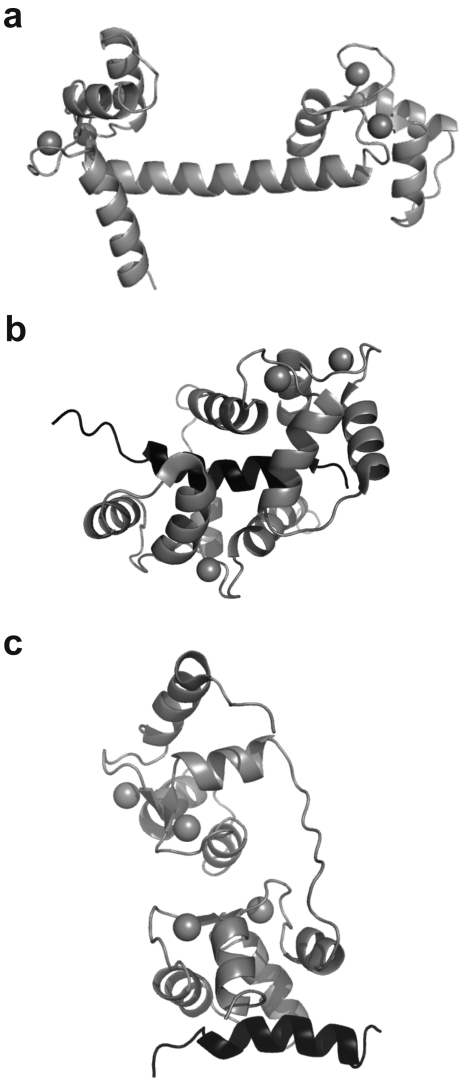

Figure 1. Three-dimensional structures of (a) $Ca^{2+}{}_4$CaM, with spheres indicating calcium ions (PDB 1CLL);[71] (b) $Ca^{2+}{}_4$CaM (gray) bound to a peptide target (black) in a collapsed conformation (PDB 2BBM);[18] and (c) $Ca^{2+}{}_4$CaM (gray) bound to a peptide target (black) in an extended conformation (PDB 1CFF).[13]

lobe in an α-helical conformation, again a process largely driven by hydrophobic interactions (Figure 1c).[13] A number of different CaM/peptide complexes have been shown to adopt this conformation, or some variant of it.[14]

Evidence suggests that the amphibian peptides inhibit NO production by interacting with CaM (reviewed by Doyle et al.[5]). This includes in vitro studies where dose−response curves showed a Hill slope greater than 1, indicating a noncompetitive interaction is causing nNOS inhibition. Also, it has been shown that the addition of excess CaM is able to partially rescue nNOS activity in an amphibian peptide treated sample, and that these peptides also inhibit the function of calcineurin, another CaM regulated enzyme.[5] Finally, NMR and MS data have shown that the peptides complex with CaM in a high-affinity fashion.[22,23] Together, these data suggest that attenuation of NO production is achieved by the peptide binding to CaM, rendering the protein unable to associate with nNOS and trigger NO synthesis.

The nNOS inhibitory peptides isolated thus far can be divided into three groups based on their common structural

Table 1. nNOS Inhibition Activities of Selected Amphibian Peptides and Synthetic Derivatives

name	sequence	IC_{50} (μM)	ref
caerin 1 peptides			
caerin 1.1	GLLSVLGSVAKHVLPHVVPVIAEHL(NH_2)	36.6	22
caerin 1.8	GLFKVLGSVAKHLLPHVVPVIAEKL(NH_2)	1.7	22
caerin 1.8.11	GLFKVLGSVAK(NH_2)	3.3	3
citropin/aurein peptides			
citropin 1.1	GLFDVIKKVASVIGGL(NH_2)	8.2	22
citropin 1.1 (mod. 13)	GLFDVIKKVASVIKKL(NH_2)	2.0	24
aurein 2.3	GLFDIVKKVVGIAGSL(NH_2)	1.8	22
dahlein/frenatin peptides			
dahlein 5.1	GLLGSIGNAIGAFIANKLKP	3.2	22
dahlein 5.6	GLLASLGKVFGGYLAEKLKPK	1.6	72
frenatin 3	GLMSVLGHAVGNVLGGLFKPKS	6.8	22

elements (Table 1). The first of these, the caerin 1 peptides, adopt a helix-hinge-helix structure.[24,25] Second are the citropin/aurein peptides, which are short linear amphipathic α-helices, and third are the dahlein/frenatin type peptides which have a characteristic C-terminal free acid and a Lys-X-Lys motif near their C-terminus.[2,3] A number of other peptides have also been isolated which cannot be categorized by this classification system.[5]

Integrated approaches to structural biology, combining data from complementary techniques, is becoming increasingly common to overcome challenges associated with individual methods. In this work, the complementary techniques of isothermal titration calorimetry (ITC) and ion mobility-mass spectrometry (IM-MS) were used to afford low resolution structural information about the complexes formed between $Ca^{2+}{}_4$CaM and the amphibian peptides caerin 1.8, caerin 1.8.11, citropin 1.1 (mod. 13), and dahlein 5.6 (Table 1). These peptides represent each of the three classes of nNOS active amphibian peptides. Caerin 1.8 is among the most potent nNOS inhibitor identified to date, while caerin 1.8.11 was investigated as it is the smallest fragment of caerin 1.8 which retains significant nNOS inhibition activity, with previous nuclear magnetic resonance spectroscopy (NMR) data indicating that the C-terminal portion of the peptide does not interact with CaM.[5] Citropin 1.1 (mod. 13) was chosen for study over the natural peptide due to its enhanced activity (likely due to the additional positive charge)[24] and dahlein 5.6 was chosen as it has comparable nNOS activity and charge to the other peptides. NMR data has previously shown that the entire dahlein 5.6 sequence interacts with CaM.[5] The strong caerin 1.8.11 interaction was further studied by NMR spectroscopy. Combined, these data from several low-resolution techniques provide significant insight into the mechanism by which these peptides interact with $Ca^{2+}{}_4$CaM, in terms of the strength of the interactions and indicate that a global conformational change in $Ca^{2+}{}_4$CaM occurs, meaning the complexes are of the canonical type. A basic insight into the mechanism of action of these peptides, and others isolated from the amphibian skin, is pivotal in determining the underling mechanism of the amphibian host defense system, and to understand how these animals survive in their natural habitat.

DOI: 10.1021/bi5004124
Biochemistry 2015, 54, 567−576

EXPERIMENTAL SECTION

Materials. Unless specified, reagents were purchased from Sigma-Aldrich (St. Louis, MO). ^{15}N-Ammonium chloride and ^{13}C-glucose were purchased from Cambridge Isotope Laboratories (Andover, MA). Peptides were synthesized using L-amino acids and the standard *N*-α-Fmoc methodology by GenScript Corp. (Piscataway, NJ). Samples for NMR spectroscopy were shown to be greater than 90% pure by HPLC and ESI-MS.

Expression and Purification of Calmodulin. CaM was expressed by inoculating Lurea broth (LB, 1% bacto-tryptone, 0.5% yeast extract, 1% sodium chloride, adjusted to pH 7) (10 mL) with a single colony of the BL21 (DE3) strain of *E. coli* containing the pET28 vector with the CaM gene inserted. This was incubated overnight at 37 °C, with shaking. A 3% subculture was made the following morning into LB and the cells were grown until an OD_{600} of 0.6−0.8 was reached. Protein expression was induced by adding IPTG to a concentration of 50 mM. The cells were left to express for 2 h before being harvested by centrifugation at 3000*g* for 15 min at 4 °C. Cell pellets were frozen at −20 °C until required.

^{15}N/^{13}C-Labeled CaM was prepared by inoculating Min A medium (60 mM dipotassium phosphate, 33 mM potassium dihydrogen phosphate, 1.7 mM sodium citrate, autoclaved, then added 15 mM ^{15}N-ammonium chloride, 0.005% thiamine, 0.2% ^{13}C-glucose, 0.8 mM magnesium sulfate, 10 mL) with a single colony of the BL21 (DE3) strain of *E. coli* containing the pET28 vector with the CaM gene inserted. This was incubated overnight at 37 °C, with shaking. A 3% subculture was made the following morning into Min A medium containing ^{15}N-ammonium chloride and ^{13}C-glucose as the sole nitrogen and carbon sources. Protein expression was completed as described above. CaM was purified using a procedure previously outlined.[26−28]

Isothermal Titration Calorimetry. CaM was extensively dialyzed against the ITC buffer (10 mM HEPES, pH 7.5, 100 mM NaCl, 10 mM $CaCl_2$) to ensure complete buffer exchange. The concentration of CaM was determined spectrophotometrically by measuring the absorbance at 277 nm and using an extinction coefficient of 3300 $M^{-1}\cdot cm^{-1}$.[29] Peptide stock solutions were prepared in Milli-Q water and concentrations determined by amino acid analysis. Aliquots were taken and lyophilized before being resuspended in the ITC buffer prior to analysis. Binding of the peptides to $Ca^{2+}{}_4$CaM was studied using a VP-ITC microcalorimeter (MicroCal, Norhampton, MA). The peptide solutions (300 μM) were injected into the sample cell containing CaM (30 μM). The first injection (2 μL) was followed by 19 injections of the peptide solution (15 μL). Experiments were conducted at four different temperatures (303.15, 308.15, 313.15, and 318.15 K for dahlein 5.6 and caerin 1.8.11, and 298.15, 303.15, 308.15, and 313.15 K for citropin 1.1 (mod. 13)). The heat of dilution was measured by titrating buffer into the protein solution and was found to be minimal, nonetheless this was subtracted from the experimental data (not shown). The raw data were fitted to a single site binding model using Origin software (version 5.0, MicroCal).

Ion Mobility-Mass Spectrometry. Bovine CaM (Sigma-Aldrich, MO) was dissolved in water at a concentration of 40 μM and dialyzed against 4x 2L 10 mM ammonium acetate, 2 mM EDTA; 4x 2L 10 mM ammonium acetate, pH 6.8. The concentration of CaM was determined spectrophotometrically by measuring the absorbance at 277 nm and using an extinction coefficient of 3300 $M^{-1}\cdot cm^{-1}$,[29] and the solution was diluted to a final concentration of 10 μM.

$Ca^{2+}{}_4$CaM was prepared by adding 2.5 mol equiv of Ca^{2+} ions in the form of calcium acetate (from a stock solution of 5 mM calcium acetate in 10 mM ammonium acetate, pH 6.8) to observe CaM with its full complement of four Ca^{2+} ions. Peptide solutions were prepared by dissolving the solid in buffer (10 mM ammonium acetate, pH 6.8) at a concentration of 1−3 mM. Small aliquots were added to the CaM solutions to achieve the desired peptide/CaM molar ratios (typically 1:1).

IM-MS spectra were acquired on a Synapt HDMS system (Waters, Manchester, U.K.),[30] using nanoESI in the positive ion mode. The sample was introduced using platinum-coated borosilicate capillary needles prepared in-house. Instrument parameters were optimized to remove adducts while preserving noncovalent interactions, and were typically as follows: capillary voltage, 1.8 kV; cone voltage, 40−80 V; trap collision energy, 10 V; source temperature, 50 °C; backing pressure, 5 mbar; IMS cell pressure (N_2), 0.5 mbar; traveling wave velocity, 400 ms^{-1}; traveling wave height, 6−9 V. The MS data were processed using the program MassLynx (Waters, Manchester, U.K., version 4.1) and deconvoluted using the maximum entropy algorithm incorporated in the software.

Drift-time measurements obtained from the Synapt HDMS were normalized for charge state and a nonlinear correction function was applied for calibrant ions such that their relative differences mirror those previously observed for the same ions.[31−34] Collision cross sections (CCSs) of the reference samples were taken from the literature using values for ubiquitin, myoglobin and cytochrome c.[35] The CCS calibration procedure is described in detail elsewhere.[34] An estimate of the error in CCS measurement is 8−10%.[34] CCSs of model protein structures were calculated using the projection approximation (PA) by means of the program MOBCAL,[36,37] and a correction function was applied to convert these to projection superposition approximation (PSA) values, as previously outlined.[38] Structural coordinates from previous studies using NMR and X-ray crystallography were obtained from the Protein Data Bank (PDB) with accession numbers indicated in the text.

Sample Preparation for NMR Titration. ^{15}N/^{13}C-Labeled CaM (3.16 mg, 1.89 nmol) was dissolved in a 500 μL aqueous solution of 10% D_2O, potassium chloride (100 mM), and calcium chloride (40 mM). The solution was adjusted to pH 6.3 by the addition of small quantities of dilute hydrochloric acid or sodium hydroxide, as required. Sodium azide (0.02%) was added as a preservative. Caerin 1.8.11 (1.69 mg, 1.51 μmol) was dissolved in water (500 μL) and divided into seven aliquots such that successive additions would give the desired mole ratio of peptide/$Ca^{2+}{}_4$CaM (0.2:1, 0.4:1, 0.6:1, 0.8:1, 1:1, 2:1, 4:1). The aliquots were lyophilized, and the dried peptide portions were added to the solution in sequence prior to recording each spectrum. The pH was readjusted to 6.3 as required.

All NMR spectra were recorded on a Varian Inova-600 NMR spectrometer with a ^{1}H frequency of 600 MHz and a ^{13}C frequency of 150 MHz. Experiments were conducted at 25 °C. The ^{1}H frequency domain was referenced to DSS at 0.0 ppm, while the heteronuclear dimensions were referenced indirectly.[39]

For ^{15}N−^{1}H HSQC spectra, the standard gNhsqc[40] pulse sequence from the VnmrJ library was used. 128 increments, each consisting of 8 transients were acquired over 2048 data points. In the ^{1}H dimension, a spectral width of 12 019.2 Hz was used, while in the ^{15}N dimension, a spectral width of

DOI: 10.1021/bi5004124
Biochemistry 2015, 54, 567−576

1944.3 Hz was used. For backbone assignment, the standard gHN_CACB[41] and gCBCA_CO_NH[42] pulse sequences from the VnmrJ library were used. Both spectra were acquired with 64 (t1) and 32 (t2) complex points, each consisting of 8 transients over 2048 data points. The carrier frequencies for ^{1}H, ^{13}C, and ^{15}N were set to 4.773, 47.362, and 118.861 ppm, respectively, and spectral widths of 12 019.2 Hz (^{1}H), 12 062.0 Hz (^{13}C) and 1944.3 Hz (^{15}N) were used. The spectra were processed using NMRPipe[43] and viewed with CCPNMR Analysis (version 2.1).[44] Assignment of the three-dimensional NMR spectra was performed using a combination of the main-chain directed[45] and sequential[46] assignment procedures. Amide chemical shift perturbations (CSPs) were calculated using eq 1, as previously described.[47]

$$\text{CSP (ppm)} = \sqrt{0.102\Delta\delta(^{15}N)^2 \; \Delta\delta(^{1}H)^2} \qquad (1)$$

RESULTS

Isothermal Titration Calorimetry. ITC was employed to determine thermodynamic parameters for the binding events between $Ca^{2+}{}_4$CaM and three amphibian peptides, namely caerin 1.8.11, citropin 1.1 (mod. 13) and dahlein 5.6. Each titration was repeated at four different temperatures and the enthalpy change of the interaction (ΔH) was determined at each temperature. Figure 2 displays representative binding data for the interaction of caerin 1.8.11 with $Ca^{2+}{}_4$CaM at 40 °C. Corresponding data for the interactions with citropin 1.1 (mod. 13) and dahlein 5.6 are shown in Supporting Information Figures 1 and 2, respectively. In all cases, the enthalpy of dilution was subtracted by performing a buffer into protein control experiment (data not shown).

Table 2 displays the thermodynamic parameters obtained by curve fitting to the measured data. The data were fit using a single site binding model and in all cases indicate a 1:1 stoichiometry of binding, with fitted stoichiometries between 0.97 and 1.23 for all titrations. In the case of citropin 1.1 (mod. 13), at low temperatures, the binding reaction is endothermic, becoming exothermic with increasing temperatures. A large favorable entropy change drives the binding interaction at lower temperatures. The interactions of caerin 1.8.11 and dahlein 5.6 with $Ca^{2+}{}_4$CaM are driven by large, favorable enthalpy changes at all the tested temperatures. This is consistent with other calorimetric studies of $Ca^{2+}{}_4$CaM binding.[48−50] The steepness of the binding curves mean that the fitted dissociation constants may not be reliable, but they were all within the range of 20−70 nM, showing that these binding events are extremely tight (Table 2).

After plotting ΔH as a function of temperature (Figure 2, Supporting Information Figures 1 and 2), the heat capacity change upon binding (ΔC_p) was estimated by measuring the slope of the resultant graph, and is used to provide information about the binding mechanism.[50] Table 2 displays the estimated ΔC_p values for the binding event between $Ca^{2+}{}_4$CaM and the studied amphibian peptides. The comparable ΔC_p values measured for the three peptide systems studied indicate a common binding mechanism. Errors in values of the ΔC_p were estimated using the errors in the linear fits of the ΔH versus T plots.

Ion Mobility-Mass Spectrometry. To gain further insight into changes in the conformations of the amphibian peptide/CaM complexes, IM-MS studies were performed to determine the collision cross section (CCS) of the complexes. CaM, and

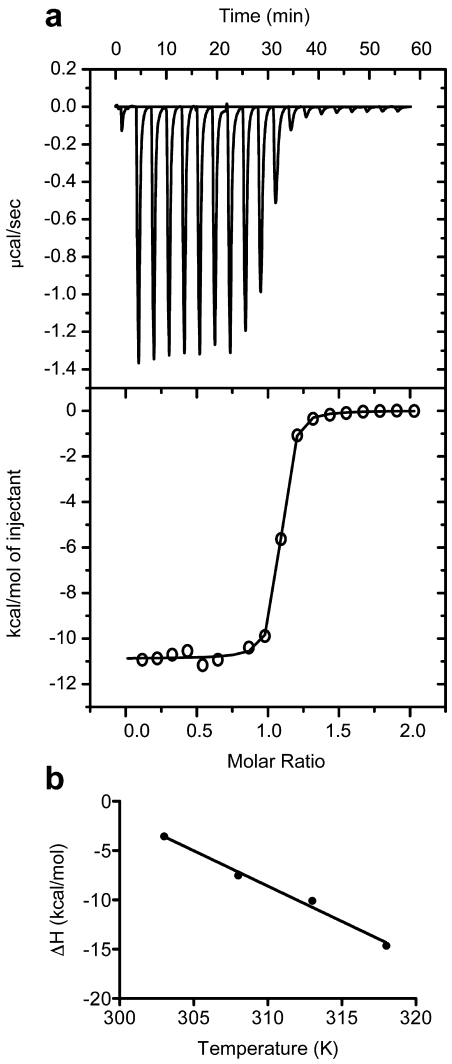

Figure 2. Calorimetric analysis of the binding of caerin 1.8.11 to $Ca^{2+}{}_4$CaM. (a) Top panel: Calorimetric titration at 40 °C. Lower panel: Binding isotherm obtained by integrating the above data. (b) Plot of ΔH as a function of temperature.

Ca^{2+} binding to the protein, has been extensively studied previously by both MS and IM-MS;[23,51−54] consequently, this paper will focus solely on the analysis of the peptide bound complexes.

Complexes of $Ca^{2+}{}_4$CaM with the amphibian peptides caerin 1.8, caerin 1.8.11, citropin 1.1 (mod. 13), and dahlein 5.6 were investigated by IM-MS, as shown in Figure 3. In addition, the complex of $Ca^{2+}{}_2$CaM with the 20 residue binding domain (C20W, LRRGQILWFRGLNRIQTQIK) of the plasma membrane Ca^{2+} pump (sequence shown below) was studied as it is known to adopt the extended conformation.[13] In all cases, the complexes studied here exhibited a 1:1 stoichiometric ratio with CaM, and at least four Ca^{2+} ions required for binding, except for C20W in which only two Ca^{2+} ion were necessary (Supporting Information Table 1). It is evident from the narrow charge state distributions of the protein complexes that they are much more well-defined in structure than apo-CaM or $Ca^{2+}{}_4$CaM, which has been shown to adopt a variety of charge states.[55] The strength of these interactions (as indicated from the presented ITC data) indicates that there should be minimal free CaM observed in the IM-MS spectra. However, as the

DOI: 10.1021/bi5004124
Biochemistry 2015, 54, 567−576

Table 2. Thermodynamic Parameters for the Titrations of Ca^{2+}_4CaM with Three Bioactive Amphibian Peptides

peptide	T (K)	K_d (nm)	ΔH (kcal/mol)	$-T\Delta S$ (kcal/mol)	n	ΔC_p (kJ/mol/K)
caerin 1.8.11	303.15	30 ± 8	−3.56 ± 0.03	−6.9	1.03	−3.00 ± 0.21
	308.15	50 ± 10	−7.52 ± 0.06	−2.8	1.05	
	313.15	40 ± 6	−10.88 ± 0.06	0.23	1.04	
	318.15	30 ± 2	−14.64 ± 0.03	3.8	1.04	
citropin 1.1 (mod. 13)	298.15	70 ± 20	3.89 ± 0.08	−12.2	1.23	−2.71 ± 0.15
	303.15	60 ± 20	0.59 ± 0.01	−9.2	0.91	
	308.15	20 ± 4	−3.32 ± 0.02	−7.6	0.97	
	313.15	50 ± 20	−5.65 ± 0.05	−4.8	1.09	
dahlein 5.6	303.15	30 ± 4	−2.55 ± 0.04	−9.2	1.11	−2.87 ± 0.09
	308.15	20 ± 6	−5.88 ± 0.05	−5.1	1.07	
	313.15	10 ± 3	−9.72 ± 0.05	−1.6	0.99	
	318.15	30 ± 9	−12.71 ± 0.14	1.7	1.10	

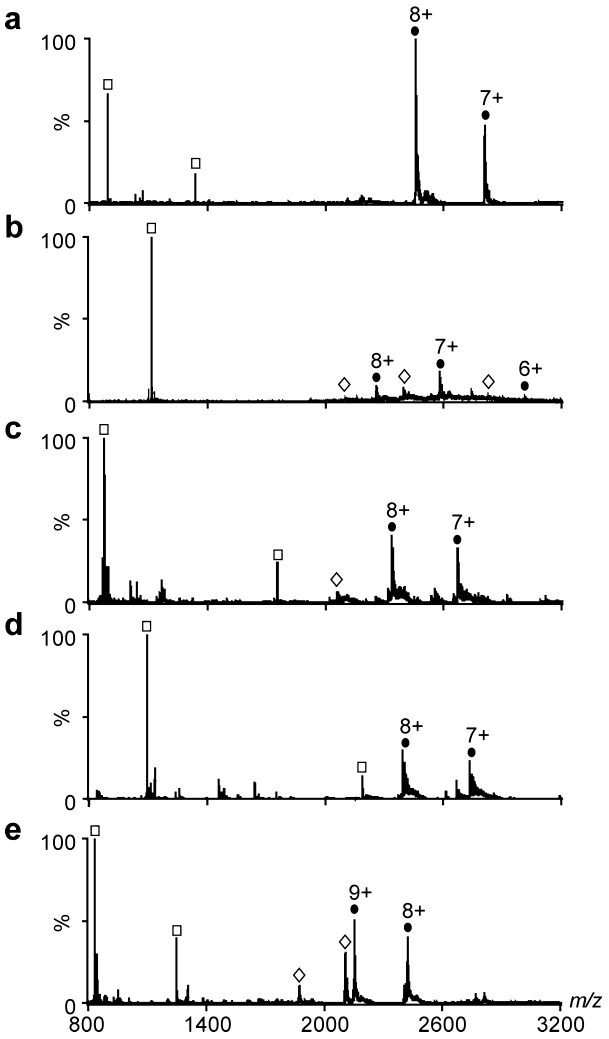

Figure 3. Mass spectra of Ca^{2+}CaM with (a) caerin 1.8, (b) caerin 1.8.11, (c) citropin 1.1 (mod. 13), (d) dahlein 5.6, and (e) plasma pump C20W. Free peptide (□); free CaM (◇); peptide/CaM complexes (●).

complexation of these peptides with CaM is dependent on hydrophobic interactions which are significantly weakened in the gas phase, it is likely that dissociation may occur upon desolvation or because of ion heating.[56,57]

Arrival time distributions (ATDs) were extracted from the spectra for Ca^{2+}_nCaM/peptide complexes (Supporting Information Figure 3), and the drift times were converted to CCS.[34] With the resolving power of both IM and MS, it is possible to selectively analyze ATDs and hence determine CCSs of ions of a particular metal bound state. In this way, we ensure the data presented is from an appropriately Ca^{2+} metalated species. The ATDs observed in these experiments were much narrower than those previously published of CaM and its Ca^{2+} adducts.[53,58] This indicates the structures of the complexes are less variable than those of CaM and that the complexes populate a more consistent structural ensemble. The calibrated CCSs are shown in Table 3.

Table 3. Experimental Collision Cross Sections for Ca^{2+}CaM/peptide Complexes as a Function of Charge State, and Estimated CCSs from Structures in the PDB

	CCS (Å^2)				
Ca^{2+}CaM/peptide complex	7+	8+	9+	protein/ complex	calculated CCS (Å^2)
caerin 1.8	2211	2191	–	CaM/NR1C1 (collapsed)[69]	1741
caerin 1.8.11	2022	2036	–	CaM/MLCK (collapsed)[18]	2194
dahlein 5.6	2136	2134	–	CaM/CaMKK (collapsed)[21]	1926
citropin 1.1 (mod. 13)	2085	2096	–	CaM/C20W (extended)[13]	2314
plasma pump C20W	–	2186	2212	apoCaM[70]	2008
				Ca^{2+}_4CaM (dumbbell)[71]	2002
				Ca^{2+}_4CaM (globular)[68]	1598

Theoretical CCSs of high resolution protein structures were calculated using coordinates in the PDB, for comparison with experimental values.[36−38] The calculated CCSs of complexes with known three-dimensional structures along with several conformational states of CaM are shown in Table 3. These values compare favorably with those determined experimentally in this work for the Ca^{2+}CaM/amphibian peptide complexes which do not have high resolution structures available. Additionally, the experimentally determined values presented in Table 3 compare well with previously determined CCSs of canonical collapsed CaM complexes by conventional drift tube

DOI: 10.1021/bi5004124
Biochemistry 2015, 54, 567−576

IM, which permits CCS determination without the use of a calibration procedure.[53]

Nuclear Magnetic Resonance Spectroscopy. In order to further investigate the nature of the noncovalent complex that forms between Ca^{2+}_4CaM and caerin 1.8.11, titration experiments were performed by adding small quantities of unlabeled caerin 1.8.11 to ^{15}N-labeled Ca^{2+}_4CaM. After each addition, a ^{15}N−^{1}H HSQC spectrum was recorded and chemical shift changes were monitored by overlaying the processed spectra (Figure 4).

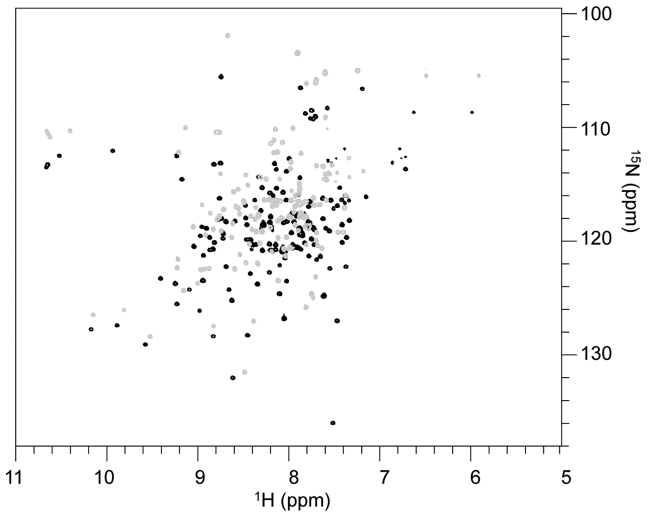

Figure 4. Overlaid ^{15}N HSQC spectra of ^{15}N-labeled Ca^{2+}_4CaM (gray) and after the addition of 1 mol equiv of caerin 1.8.11 (black). Assignments for the spectra of caerin 1.8.11 bound to Ca^{2+}_4CaM are detailed in Supporting Information Table 2.

It is apparent that significant chemical shift changes occur for most residues in the titration, suggesting a global reorganization of protein structure. This is consistent with the complex adopting the canonical collapsed structure. Chemical shift changes were not observed as a function of concentration; instead a second set of peaks with a different chemical shift signature corresponding to the protein-peptide complex was observed after 0.4 equiv of peptide were added (data not shown). This is consistent with the complex being in the slow exchange regime, which is consistent with a nanomolar binding affinity for the interaction. Addition of an equimolar quantity of peptide resulted in only one set of peaks being observed in the spectrum, corresponding to the complex, and addition of further peptide did not have any additional effect on the observed chemical shifts.

The structural changes in Ca^{2+}_4CaM associated with binding a peptide result in chemical shift perturbations. Consequently, these data can be used to indicate which regions of Ca^{2+}_4CaM experience significant changes in their chemical environment upon binding. A full structural analysis using NOE information would be required to determine the overall structure of Ca^{2+}_4CaM in complex with a peptide. Nevertheless, significant structural information can be obtained from the assigned backbone chemical shifts.

Ca^{2+}_4CaM is a well-studied protein that is known to have a high helical content, comprising eight α-helices separated by several loop motifs. In the X-ray structure, the central helices IV and V appear to combine into one extended helix possibly due to crystal packing effects, however, NMR and other data indicate that these are discrete structural motifs and their separation results in a centrally located flexible hinge region.[59,60] The known helical regions are indicated by the shaded portions in Figure 5.

Figure 5a displays ^{13}Cα secondary shifts which are a good marker for helical regions of secondary structure.[61,62] These data demonstrate the loss of helicity about the central flexible hinge region (residues 77−82), as indicated by the negative secondary shifts in this region. However, the eight helices of Ca^{2+}_4CaM are largely retained upon binding to caerin 1.8.11, indicated by the eight sustained regions of positive secondary

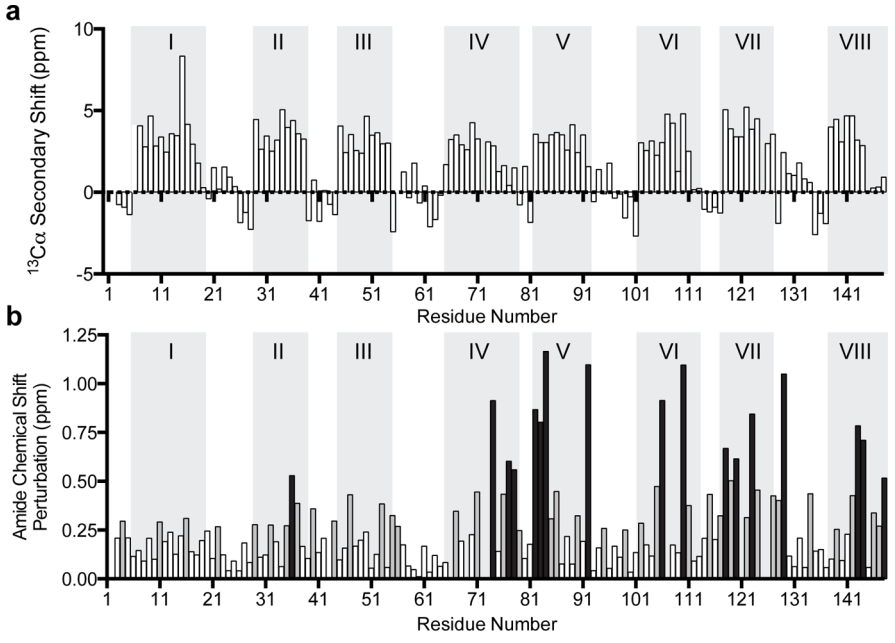

Figure 5. (a) αC ^{13}C secondary shifts of Ca^{2+}_4CaM bound to caerin 1.8.11. (b) Average amide CSP in Ca^{2+}_4CaM as a result of binding to caerin 1.8.11. CSPs > 0.25 are described as significant (gray), and CSPs > 0.5 are described as dramatic (black).[65]

DOI: 10.1021/bi5004124
Biochemistry 2015, 54, 567−576

shifts. This demonstrates that the large chemical shift changes observed as a result of binding are likely due to rearrangement of the helices, rather than a dissolution of any secondary structure elements.

It is possible to map chemical shift perturbations (CSPs) that occur in $Ca^{2+}{}_4$CaM upon complexation with caerin 1.8.11, to determine regions where significant CSPs occur as a result of binding. These data essentially depict the difference in chemical shift between the unbound and bound forms of $Ca^{2+}{}_4$CaM. To obtain a clear, overall picture of the CSPs that are occurring upon binding to caerin 1.8.11, Figure 5b displays the overall CSPs of the amide groups of the protein.[47] There are significant CSPs across the protein backbone, but generally speaking, the most dramatic perturbations are observed in the central region of the protein (around residue 81) and at the C-terminus.

DISCUSSION

Structural biology allows for mechanistic insight into the processes which underlie biological function at a molecular level. Typically, however, limitations in individual methods mean an integrated approach is often necessary to offer a more complete description of the system of interest, and take advantage of complementary information provided by different structural biology techniques. The purpose of this study was to further characterize the interactions of several bioactive amphibian peptides with $Ca^{2+}{}_4$CaM utilizing a combination of low resolution structural biology approaches. The mechanism by which these peptides inhibit NO production is of particular scientific interest, as a rigorous host-defense system is important to the survival of amphibian populations. In this work, we used ITC to measure thermodynamic parameters of the binding event, which was used to elucidate a binding mode. MS was used to determine the stoichiometry of the interactions, and IM-MS was used to gain information about the conformation of the bound species. Finally, NMR spectroscopy was combined with CSP analysis to provide further support for the binding mode determined by the other two low resolution techniques. Combined, the data presented herein from these complementary low resolution technologies. suggests that $Ca^{2+}{}_4$CaM binds in a similar mode to the range of amphibian peptides studied, which share little sequence homology, demonstrating the inherent flexibility in $Ca^{2+}{}_4$CaM binding specificity.

Isothermal Titration Calorimetry. The ΔC_p values of binding have been determined (Table 2), with these values lying in the range of −2.7 to −3.0 kJ/mol/K. A number of $Ca^{2+}{}_n$CaM/peptide complexes have been previously studied by ITC, and their associated ΔC_p values have been reported.[50] The previously studied peptides were divided into two groups, depending on the ΔC_p of their complexation reaction with $Ca^{2+}{}_4$CaM. It has been determined that a complex which adopts the canonical collapsed conformation exhibits a ΔC_p in the order of −3.2 kJ/mol/K, while extended conformations, where only the C-terminal lobe of $Ca^{2+}{}_n$CaM is involved in binding, exhibit a ΔC_p in the order of −1.6 kJ/mol/K.[50] This significant difference in magnitude can be attributed to the decreased solvent accessible surface area when the complex adopts the canonical collapsed conformation. Comparison of the results obtained here with the previously determined ΔC_p values lends support to the notion that the studied amphibian peptides cause $Ca^{2+}{}_4$CaM to adopt the canonical collapsed conformation upon binding, with the peptide encapsulated between the N- and C- terminal lobes of the protein.

The strength of these interactions mean ITC could not be used to accurately determine kinetic parameters for these binding interactions. Nevertheless, the data presented here demonstrates that the interactions between the amphibian peptides and $Ca^{2+}{}_4$CaM are very strong, with approximated K_d values in the low nanomolar range.

Ion Mobility-Mass Spectrometry. This work presents the first example of IM-MS analysis of $Ca^{2+}{}_4$CaM/amphibian peptide complexes. It can be seen in Figure 3 that the charge state distributions of the CaM/peptide complexes are relatively narrow and are at low charge states (high m/z), suggesting the complexes are of well-defined structure. This is distinct from the conformational flexibility in apo- and holo-CaM, and the consequent large number of charge states observed previously.[23,51−54] Additionally, it can be seen that the $Ca^{2+}{}_4$CaM/amphibian peptide complexes adopt charge states of $[M + 8H]^{8+}$ and $[M + 7H]^{7+}$, while the $Ca^{2+}{}_2$CaM/C20W complex, which has been shown by NMR to adopt the less common extended conformation,[13] adopts charge states $[M + 8H]^{8+}$ and $[M + 9H]^{9+}$ (Figure 3). The higher charge states adopted by the CaM/C20W complex is consistent with it having a more extended structure than the other complexes studied.

The calibrated CCSs for the complexes studied at the charge states observed are summarized in Table 3. Comparison of the measured CCSs at the $[M + 8H]^{8+}$ charge state observed for all complexes demonstrate that, generally speaking, the $Ca^{2+}{}_4$CaM/amphibian peptide complexes exhibit smaller CCSs than that of the $Ca^{2+}{}_4$CaM/C20W complex. This is consistent with these complexes adopting the more compact, canonical structure upon binding. Notably, the $Ca^{2+}{}_4$CaM/caerin 1.8 and $Ca^{2+}{}_4$CaM/C20W complexes have comparable CCS's, which are larger than the CaM complex with the truncated variant caerin 1.8.11. Isotope labeling combined with NMR and chemical shift analysis has previously shown that only the N-terminal portion of caerin 1.8 is encapsulated by CaM, with the remaining C-terminal region excluded from the binding pocket.[5] The slightly larger CCS of the $Ca^{2+}{}_4$CaM/caerin 1.8 complex is explained by these data, with the remaining peptide excluded from the complex, so it is unstructured and flexible in solution resulting in a larger CCS.

Conversely, previously reported chemical shift perturbation data has indicated that the entirety of the dahlein 5.6 peptide interacts with $Ca^{2+}{}_4$CaM,[63] and is encapsulated by the protein, providing an explanation as to why the complex has a smaller CCS than that involving caerin 1.8. Similar experiments have not been performed for citropin 1.1 (mod. 13), although the measured CCS lies between those of the caerin 1.8.11 and dahlein 5.6 complexes, suggesting that the peptide is completely engulfed within $Ca^{2+}{}_4$CaM upon complexation.

Theoretical CCSs were calculated for model canonical compact and extended complex structures (Table 3). These theoretical CCSs demonstrate that the canonical collapsed complex structures exhibit a reasonable variation in CCS. However, it is clearly evident that the $Ca^{2+}{}_2$CaM/C20W complex exhibits a larger CCS, consistent with its extended conformation, where only one lobe of CaM is involved in binding the peptide. Comparison of the theoretical CCS of the $Ca^{2+}{}_2$CaM/C20W complex with those measured from IM-MS show a good agreement between the two. In addition, CCSs of the amphibian peptide complexes all show good agreement with those calculated from structures in the PDB which adopt the compact conformation (except for the caerin 1.8 complex, due to the reasons outlined above), as well as the CCSs of other

DOI: 10.1021/bi5004124
Biochemistry 2015, 54, 567−576

complexes with collapsed structures determined previously by drift tube IM-MS.[53] This provides further support for the notion that these Ca^{2+}_4CaM/amphibian peptide complexes are of this canonical structure.

Nuclear Magnetic Resonance Spectroscopy. It is well documented that peptide binding to Ca^{2+}_4CaM results in minimal disruption to the helical structure of the protein.[14,64−66] It is apparent from the NMR data that a similar situation is observed here for the complex of Ca^{2+}_4CaM with caerin 1.8.11. This complex was chosen for further study due to its stability and the relatively small size of the peptide required for binding to Ca^{2+}_4CaM. The eight sustained regions of downfield αC ^{13}C secondary shifts, as indicated in Figure 5, conform with the known eight helices as determined by NMR studies of the unbound Ca^{2+}_4CaM[60] and are largely unchanged upon the global reorganization of protein structure with peptide binding. These data are also consistent with previous observations that the central helix of Ca^{2+}_4CaM, as observed in the X-ray crystal structure, is disrupted at the known hinge region in solution (residues K77-E82).[59,60] This flexible hinge is necessary for the conformational rearrangement that occurs when binding peptide targets in the canonical compact conformation.

In addition, while the data obtained from NMR again supports the notion that the whole protein is involved in binding, the enhanced CSPs at the C-terminus suggest the peptide more strongly associates with this region (Figure 5), as outlined for several other CaM binding peptides which adopt the canonical complex structure.[65,67] These CSPs can be mapped to residues of the hydrophobic pockets of CaM, or those residues nearby (Supporting Information Figure 4). This hydrophobic core region is considered to be formed by the first and fourth helices of each domain (i.e., helices I and IV form the N-terminal hydrophobic domain and helices V and VIII form the C-terminal hydrophobic domain[68]). Notably, significant or dramatic CSPs are observed for numerous hydrophobic residues in and around the hydrophobic core region. This indicates that hydrophobic interactions are vital in the binding of Ca^{2+}_4CaM to caerin 1.8.11. Additionally, many of the Met residues located in both of the N- and C- terminal hydrophobic pockets of CaM (such as Met 36, 71, 109,124, 144, and 155) show dramatic CSPs upon binding (Figure 5 and Supporting Information Figure 4). These Met residues are well-known to play an important role in binding.[14] Together, these data indicate that both hydrophobic regions of Ca^{2+}_4CaM are involved in binding to caerin 1.8.11, confirming that the complex is adopting the canonical compact arrangement.

CONCLUSIONS

Most amphibians of the genera *Litoria* and *Crinia* that have been studied thus far produce one or more peptides that prevent NO formation by nNOS as part of their glandular secretion. It has been well-documented that these bioactive amphibian peptides bind to Ca^{2+}_4CaM inducing a further conformational change which prevents the protein from activating nNOS. In this work, the Ca^{2+}_4CaM complexes that are formed with the amphibian peptides caerin 1.8, dahlein 5.6, and citropin 1.1 (mod. 13) have been studied using a variety of complementary biophysical techniques.

ITC permitted the thermodynamic parameters of the interaction to be measured, but the kinetic parameters of the binding events could not be reliably determined. These thermodynamic parameters revealed that the peptides share a common binding mode, with a significant global structural reorganization of Ca^{2+}_4CaM resulting in the amphibian peptides being engulfed in a channel between the N- and C-terminal domains. This was further supported by the data obtained from IM-MS, with the CCSs of the observed ions correlating well with those predicted from high resolution canonical collapsed CaM complex structures. Additionally, it could be inferred that the citropin 1.1 (mod. 13) adopts a structure similar to the caerin 1.8 complex, with part of the peptide excluded from the hydrophobic cavity. This could not be determined from the ITC data. Finally, the data from NMR spectroscopy provides further evidence for a collapsed binding mode in the case of caerin 1.8.11. However, these experiments and the associated data analysis are much more labor intensive than analysis by ITC or IM-MS.

The combination of low resolution structural information presented herein from ITC, IM-MS, and NMR spectroscopy provides significant insight into the structures of both CaM and its complexes with several amphibian peptides.

ASSOCIATED CONTENT

Supporting Information

Figures showing calorimetric analysis of amphibian peptide/Ca^{2+}_4CaM interactions, ATDs measured by IM-MS and CSPs mapped on the Ca^{2+}_4CaM surface. Tables of expected and experimentally determined masses and assigned chemical shifts of the Ca^{2+}_4CaM/caerin 1.8.11 complex. This material is available free of charge via the Internet at http://pubs.acs.org.

AUTHOR INFORMATION

Corresponding Author

*Phone: +61 8 8313 5497. Fax: +61 8 8313 4380. E-mail: tara.pukala@adelaide.edu.au.

Funding

This work was supported by the Australian Research Council.

Notes

The authors declare no competing financial interest.

ACKNOWLEDGMENTS

We thank Mr Philip Clements for his help in acquiring NMR spectra.

ABBREVIATIONS

ATD, arrival time distribution; CaM, calmodulin; Ca^{2+}_nCaM, Ca^{2+}-bound CaM; Ca^{2+}_4CaM, holo-CaM; CCS, collision cross section; CSP, chemical shift perturbation; ΔC_p, heat capacity; IM-MS, ion mobility-mass spectrometry; ITC, isothermal titration calorimetry; NMR, nuclear magnetic resonance; nNOS, neuronal nitric oxide synthase; NO, nitric oxide

REFERENCES

(1) Clarke, B. T. (1997) The natural history of amphibian skin secretions, their normal functioning and potential medical applications. *Biol. Rev. 72*, 365−379.

(2) Apponyi, M. A., Pukala, T. L., Brinkworth, C. S., Maselli, V. M., Bowie, J. H., Tyler, M. J., Booker, G. W., Wallace, J. C., Carver, J. A., Separovic, F., Doyle, J., and Llewellyn, L. E. (2004) Host-defence peptides of Australian anurans: Structure, mechanism of action and evolutionary significance. *Peptides 25*, 1035−1054.

(3) Pukala, T. L., Bowie, J. H., Maselli, V. M., Musgrave, I. F., and Tyler, M. J. (2006) Host-defence peptides from the glandular secretions of amphibians: Structure and activity. *Nat. Prod. Rep. 23*, 368−393.

DOI: 10.1021/bi5004124
Biochemistry 2015, 54, 567−576

(4) Bowie, J. H., Separovic, F., and Tyler, M. J. (2012) Host-defense peptides of Australian anurans. Part 2. Structure, activity, mechanism of action, and evolutionary significance. *Peptides 37*, 174−188.
(5) Doyle, J. R., Bowie, J. H., Jackway, R. J., Llewellyn, L. E., Pukala, T. L., Apponyi, M. A., and Booker, G. W. (2009) Anuran Host-Defense Peptides That Complex with Ca^{2+} Calmodulin and Inhibit the Synthesis of the Cell Signaling Agent Nitric Oxide by Neuronal Nitric Oxide Synthase, in *Bioactive Peptides* (Howl, J., and Jones, S., Eds.), CRC Press, London.
(6) Renteria, R. C., and Constantine-Paton, M. (1999) Nitric oxide in the retinotectal system: A signal but not a retrograde messenger during map refinement and segregation. *J. Neurosci. 19*, 7066−7076.
(7) Gobbetti, A., and Zeran, M. (1999) Hormonal and cellular brain mechanisms regulating the amplexus of male and female water frog (*Rana esculenta*). *J. Neuroendocrinol. 11*, 589−596.
(8) Molero, M., Hernandez, I. M., Lobo, P., Cardenas, P., Romero, R., and Chacin, J. (1998) Modulation by nitric oxide of gastric acid secretion in toads. *Acta Physiol. Scand. 164*, 229−236.
(9) Crivici, A., and Ikura, M. (1995) Molecular and structural basis of target recognition by calmodulin. *Annu. Rev. Biophys. Biomol. Struct. 24*, 85−116.
(10) O'Neil, K. T., and DeGrado, W. F. (1990) How calmodulin binds its targets: Sequence independent recognition of amphiphilic α-helices. *Trends Biochem. Sci. 15*, 59−64.
(11) Yuan, T., Yap, K. L., and Ikura, M. (2000) Calmodulin target recognition: Common mechanism and structural diversity, in *Calcium Homeostasis* (Carafoli, E., and Krebs, J., Eds.), Springer, Berlin.
(12) Williams, R. J. P. (1992) Calcium and calmodulin. *Cell Calcium 13*, 355−362.
(13) Elshorst, B., Hennig, M., Forsterling, H., Diener, A., Maurer, M., Schulte, P., Schwalbe, H., Griesinger, C., Krebs, J., Schmid, H., Vorherr, T., and Carafoli, E. (1999) NMR solution structure of a complex of calmodulin with a binding peptide of the Ca^{2+} pump. *Biochemistry 38*, 12320−12332.
(14) Vetter, S. W., and Leclerc, E. (2003) Novel aspects of calmodulin target recognition and activation. *Eur. J. Biochem. 270*, 404−414.
(15) Contessa, G. M., Orsale, M., Melino, S., Torre, V., Paci, M., Desider, A., and Cicero, D. O. (2005) Structure of calmodulin complexed with an olfactory CNG channel fragment and role of the central linker: Residual dipolar couplings to evaluate calmodulin binding modes outside the kinase family. *J. Biomol. NMR 31*, 185−199.
(16) Wintrode, P. L., and Privalov, P. L. (1997) Energetics of target peptide recognition by calmodulin: A calorimetric study. *J. Mol. Biol. 266*, 1050−1062.
(17) Nelson, M. R., and Chazin, W. J. (1998) Calmodulin as a calcium sensor, in *Calmodulin and Signal Transduction* (Van Eldik, L. J., and Watterson, D. M., Eds.), pp 17−64, Academic Press, New York.
(18) Ikura, M., Clore, G. M., Gronenborn, A. M., Zhu, G., Klee, C. B., and Bax, A. (1992) Solution structure of a calmodulin-target peptide complex by multidimensional NMR. *Science 256*, 632−638.
(19) Meador, W. E., Means, A. R., and Quiocho, F. A. (1992) Target enzyme recognition by calmodulin: 2.4 Å structure of a calmodulin peptide complex. *Science 257*, 1251−1255.
(20) Meador, W. E., Means, A. R., and Quiocho, F. A. (1993) Modulation of calmodulin plasticity in molecular recogntition on the basis of X-ray structures. *Science 262*, 1718−1721.
(21) Osawa, M., Tokumits, H., Swindells, M. B., Kurihara, H., Orita, M., Shibanuma, T., Furuya, T., and Ikura, M. (1999) A novel target recognition revealed by calmodulin in complex with Ca^{2+}-calmodulin-dependent kinase kinase. *Nat. Struct. Biol. 6*, 819−824.
(22) Doyle, J., Llewellyn, L. E., Brinkworth, C. S., Bowie, J. H., Wegener, K. L., Rozek, T., Wabnitz, P. A., Wallace, J. C., and Tyler, M. J. (2002) Amphibian peptides that inhibit neuronal nitric oxide synthase: The isolation of lesueurin from the skin secretion of the Australian stony creek frog *Litoria lesueuri*. *Eur. J. Biochem. 269*, 100−109.
(23) Pukala, T. L., Urathamakul, T., Watt, S. J., Beck, J. L., Jackway, R. J., and Bowie, J. H. (2008) Binding studies of nNOS-active amphibian peptides and Ca^{2+} calmodulin, using negative ion ESI mass spectrometry. *Rapid Commun. Mass Spectrom. 22*, 3501−3509.
(24) Doyle, J., Brinkworth, C. S., Wegener, K. L., Carver, J. A., Llewellyn, L. E., Olver, I. N., Bowie, J. H., Wabnitz, P. A., and Tyler, M. J. (2003) nNOS inhibition, antimicrobial and anticancer activity of the amphibian skin peptide, citropin 1.1 and synthetic modification: The solution structure of a modified citropin 1.1. *Eur. J. Biochem. 270*, 1141−1153.
(25) Bowie, J. H., Chia, B. C. S., and Tyler, M. J. (1998) Host defence peptides from the skin glands of Australian amphibians: A powerful chemical arsenal. *Pharmacol. News 5*, 16−21.
(26) Majava, V., Petoukhov, M. V., Hayashi, N., Pirilä, P., Svergun, D. I., and Kursula, P. (2008) Interaction between the C-terminal region of human myelin basic protein and calmodulin: Analysis of complex formation and solution structure. *BMC Struct. Biol.*, DOI: 10.1186/1472-6807-8-10.
(27) Kursula, P., and Majava, V. (2007) A structural insight into lead neurotoxicity and calmodulin activation by heavy metals. *Acta Crystallogr. F63*, 653−656.
(28) Gopalakrishna, R., and Anderson, W. B. (1982) Ca^{2+}-induced hydrophobic site on calmodulin: application for purification of calmodulin by phenyl-Sepharose affinity chromatography. *Biochem. Biophys. Res. Commun. 104*, 830−836.
(29) Crouch, T. H., and Klee, C. B. (1980) Positive cooperative binding of calcium to bovine brain calmodulin. *Biochem. 19*, 3692−3698.
(30) Pringle, S. D., Giles, K., Wildgoose, J. L., Williams, J. P., Slade, S. E., Thalassinos, K., Bateman, R. H., Bowers, M. T., and Scrivens, J. H. (2007) An investigation of the mobility separation of some peptide and protein ions using a new hybrid quadrupole/travelling wave IMS/oa-Tof instrument. *Int. J. Mass Spectrom. 261*, 1−12.
(31) Shvartsburg, A. A., and Smith, R. D. (2008) Fundamentals of traveling wave ion mobility spectrometry. *Anal. Chem. 80*, 9689−9699.
(32) Thalassinos, K., Grabenauer, M., Slade, S. E., Hilton, G. R., Bowers, M. T., and Scrivens, J. H. (2009) Characterization of phosphorylated peptides using traveling wave-based and drift cell ion mobility mass spectrometry. *Anal. Chem. 81*, 248−254.
(33) Scarff, C. A., Thalassinos, K., Hilton, G. R., and Scrivens, J. H. (2008) Travelling wave ion mobility mass spectrometry studies of protein structure: Biological significance and comparison with X-ray crystallography and nuclear magnetic resonance spectroscopy measurements. *Rapid Commun. Mass Spectrom. 22*, 3297−3304.
(34) Ruotolo, B. T., Benesch, J. L. P., Sandercock, A. M., Hyung, S.-J., and Robinson, C. V. (2008) Ion mobility-mass spectrometry analysis of large protein complexes. *Nat. Protoc. 3*, 1139−1151.
(35) Clemmer, D. E. Cross section database, URL: http://www.indiana.edu/~clemmer/.
(36) Shvartsburg, A. A., and Jarrold, M. F. (1996) An exact hard-spheres scattering model for the mobilities of polyatomic ions. *Chem. Phys. Lett. 261*, 86−91.
(37) Mesleh, M. F., Hunter, J. M., Shvartsburg, A. A., Schatz, G. C., and Jarrold, M. F. (1996) Structural information from ion mobility measurements: Effects of the long-range potential. *J. Phys. Chem. 100*, 16082−16086.
(38) Bleiholder, C., Wyttenbach, T., and Bowers, M. T. (2011) A novel projection approximation algorithm for the fast and accurate computation of molecular collision cross sections (I). Method. *Int. J. Mass Spectrom. 308*, 1−10.
(39) Wishart, D. S., Bigam, C. G., Yao, J., Dyson, H. J., Oldfield, E., Markley, J. L., and Sykes, B. D. (1995) ^{1}H, ^{13}C and ^{15}N chemical shift referencing in biomolecular NMR. *J. Biomol. NMR 6*, 135−140.
(40) Kay, L. E., Keifer, P., and Saarinen, T. (1992) Pure absorption gradient enhanced heteronuclear single quantum correlation spectroscopy with improved sensitivity. *J. Am. Chem. Soc. 114*, 10663−10665.
(41) Wittekind, M., and Mueller, L. (1993) HNCACB, a high-sensitivity 3D NMR experiment to correlate amide-proton and nitrogen resonances with the alpha- and beta-carbon resonances in proteins. *J. Magn. Res., Ser. B 101*, 201−205.

DOI: 10.1021/bi5004124
Biochemistry 2015, 54, 567−576

(42) Grzesiek, S., and Bax, A. (1992) Correlating backbone amide and side chain resonances in larger proteins by multiple relayed triple resonance NMR. *J. Am. Chem. Soc. 114*, 6291−6293.
(43) Delaglio, F., Grzesiek, S., Vuister, G. W., Zhu, G., Pfeifer, J., and Bax, A. (1995) NMRPipe: A multidimensional spectral processing system based on UNIX pipes. *J. Biomol. NMR 6*, 277−293.
(44) Vranken, W. F., Boucher, W., Stevens, T. J., Fogh, R. H., Pajon, A., Llinas, M., Ulrich, E. L., Markley, J. L., Ionides, J., and Laue, E. D. (2005) The CCPN data model for NMR spectroscopy: Development of a software pipeline. *Proteins 59*, 687−696.
(45) Englander, S. W., and Wand, A. J. (1987) Main-chain-directed strategy for the assignment of 1H NMR spectra of proteins. *Biochem. 26*, 5953−5958.
(46) Wüthrich, K. (1986) *NMR of Proteins and Nucleic Acids*, John Wiley and Sons, New York.
(47) Schumann, F. H., Riepl, H., Maurer, T., Gronwald, W., Neidig, K. P., and Kalbitzer, H. R. (2007) Combined chemical shift changes and amino acid specific chemical shift mapping of protein-protein interactions. *J. Biomol. NMR 39*, 275−289.
(48) Myllykoski, M., Kuczera, K., and Kursula, P. (2009) Complex formation between calmodulin and a peptide from the intracellular loop of the gap junction protein connexin43: Molecular conformation and energetics of binding. *Biophys. Chem. 144*, 130−135.
(49) Tse, J. K., Giannetti, A. M., and Bradshaw, J. M. (2007) Thermodynamics of calmodulin trapping by Ca2+/calmodulin-dependent protein kinase II: Subpicomolar K_d determined using competition titration calorimetry. *Biochemistry 46*, 4017−4027.
(50) Brokx, R. D., Lopez, M. M., Vogel, H. J., and Makhatadze, G. I. (2001) Energetics of target peptide binding by calmodulin reveals different modes of binding. *J. Biol. Chem. 276*, 14083−14091.
(51) Pan, J., and Konermann, L. (2010) Calcium-induced structural transitions of the calmodulin-melittin system studied by electrospray mass spectrometry: Conformational subpopulations and metal-unsaturated intermediates. *Biochem. 49*, 3477−3486.
(52) Nemirovskiy, O., Giblin, D. E., and Gross, M. L. (1999) Electrospray ionization mass spectometry and hydrogen/deuterium exchange for probing the interaction of calmodulin with calcium. *J. Am. Soc. Mass Spectrom. 10*, 711−718.
(53) Wyttenbach, T., Grabenauer, M., Thalassinos, K., Scrivens, J. H., and Bowers, M. T. (2009) The Effect of Calcium Ions and Peptide Ligands on the Relative Stabilities of the Calmodulin Dumbbell and Compact Structures. *J. Phys. Chem. B 114*, 437−447.
(54) Faull, P. A., Korkeila, K. E., Kalapothakis, J. M., Gray, A., McCullough, B. J., and Barran, P. E. (2009) Gas-phase metalloprotein complexes interrogated by ion mobility-mass spectrometry. *Int. J. Mass Spectrom. 283*, 140−148.
(55) Kaltashov, I. A., and Abzalimov, R. R. (2008) Do ionic charges in ESI MS provide useful information on macromolecular structure? *J. Am. Soc. Mass Spectrom. 19*, 1239−1246.
(56) Loo, J. A. (1997) Studying noncovalent protein complexes by electrospray ionization mass spectrometry. *Mass Spectrom. Rev. 16*, 1−23.
(57) Robinson, C. V., Chung, E. W., Kragelund, B. B., Knudsen, J., Aplin, R. T., Poulsen, F. M., and Dobson, C. M. (1996) Probing the nature of noncovalent interactions by mass spectrometry. A study of protein-CoA ligand binding and assembly. *J. Am. Chem. Soc. 118*, 8646−8653.
(58) Calabrese, A. N., Speechley, L. A., and Pukala, T. L. (2012) Characterisation of calmodulin structural transitions by ion mobility mass spectrometry. *Aust. J. Chem. 65*, 504−511.
(59) Babu, Y. S., Bugg, C. E., and Cook, W. J. (1988) Structure of calmodulin refined at 2.2 Å resolution. *J. Mol. Biol. 204*, 191−204.
(60) Ikura, M., Spera, S., Barbato, G., Kay, L. E., Krinks, M., and A, B. (1991) Secondary structure and side-chain ^{1}H and ^{13}C resonace assignments of calmodulin in solution by heteronuclear multidimensional NMR spectroscopy. *Biochem. 30*, 9216−9228.
(61) Wishart, D. S., Sykes, B. D., and Hodges, R. S. (1991) Relationship between nuclear magnetic resonance chamical shift and protein secondary structure. *J. Mol. Biol. 222*, 311−333.
(62) Pastore, A., and Saudek, V. (1990) The relationship between chemical shift and secondary structure in proteins. *J. Magn. Reson. 90*, 165−176.
(63) Jackway, R. J., and Bowie, J. H. Unpublished observations.
(64) Hoeflich, K. P., and Ikura, M. (2002) Calmodulin in action: Diversity in target recognition and activation mechanisms. *Cell 108*, 739−742.
(65) Carlier, L., Byrne, C., Miclet, E., Bourgoin-Voillard, S., Nicaise, M., Tabet, J. C., Desmadril, M., Leclercq, G., Lequin, O., and Jacquot, Y. (2012) Biophysical studies of the interaction between calmodulin and the R287-T311 region of human estrogen receptor alpha reveals an atypical binding process. *Biochem. Biophys. Res. Commun. 419*, 356−361.
(66) Shi, Q., Wang, X., and Ren, J. (2008) Biophysical characterization of the interaction of p21 with calmodulin: a mechanistic study. *Biophys. Chem. 138*, 138−143.
(67) Ikura, M., Kay, L. E., Krinks, M., and Bax, A. (1991) Triple-resonance multidimensional NMR study of calmodulin complexed with the binding domain of skeletal muscle myosin light-chain kinase: Indication of conformational change in the central helix. *Biochemistry 50*, 5498−5504.
(68) Fallon, J. L., and Quiocho, F. A. (2003) A closed compact structure of native Ca^{2+}-calmodulin. *Structure 11*, 1303−1307.
(69) Ataman, Z. A., Gakhar, K., Sorensen, B. R., Hell, J. W., and Shea, M. A. (2007) The NMDA receptor NR1 C1 region bound to calmodulin: Structural insights into functional differences between homologous domains. *Structure 15*, 1603−1617.
(70) Zhang, M., Tanaka, T., and Ikura, M. (1995) Calcium-induced conformational transition revealed by the solution structure of apo calmodulin. *Nat. Struct. Biol. 2*, 758−767.
(71) Chattopadhyaya, R., Meador, W. E., Means, A. R., and Quiocho, F. A. (1992) Calmodulin structure refined at 1.7 Å resolution. *J. Mol. Biol. 228*, 1177−1192.
(72) Brinkworth, C. S., Carver, J. A., Wegener, K. L., Doyle, J., Llewellyn, L. E., and Bowie, J. H. (2003) The solution structure of frenatin 3, a neuronal nitric oxide synthase inhibitor from *Litoria infrafrenata*. *Biopolymers 70*, 424−434.

DOI: 10.1021/bi5004124
Biochemistry 2015, 54, 567−576